Virial expansion for almost diagonal random matrices

2003 J. Phys. A: Math. Gen. 36 8265

(http://iopscience.iop.org/0305-4470/36/30/305)

INSTITUTE OF PHYSICS PUBLISHING JOURNAL OF PHYSICS A: MATHEMATICAL AND GENERAL

J. Phys. A: Math. Gen. **36** (2003) 8265–8289 PII: S0305-4470(03)62855-6

Virial expansion for almost diagonal random matrices

Oleg Yevtushenko[1] **and Vladimir E Kravtsov**[1,2]

[1] The Abdus Salam ICTP, Strada Costiera 11, 34100, Trieste, Italy
[2] Landau Institute for Theoretical Physics, 2 Kosygina st., 117940 Moscow, Russia

E-mail: bom@ictp.trieste.it and kravtsov@ictp.trieste.it

Received 25 April 2003
Published 16 July 2003
Online at stacks.iop.org/JPhysA/36/8265

Abstract

Energy level statistics of Hermitian random matrices $\hat{H}$ with Gaussian independent random entries $H_{i\geqslant j}$ is studied for a generic ensemble of almost diagonal random matrices with $\langle|H_{ii}|^2\rangle \sim 1$ and $\langle|H_{i\neq j}|^2\rangle = b\mathcal{F}(|i-j|) \ll 1$. We perform a regular expansion of the spectral form-factor $K(\tau) = 1 + bK_1(\tau) + b^2K_2(\tau) + \cdots$ in powers of $b \ll 1$ with the coefficients $K_m(\tau)$ that take into account interaction of $(m+1)$ energy levels. To calculate $K_m(\tau)$, we develop a diagrammatic technique which is based on the Trotter formula and on the combinatorial problem of graph edges colouring with $(m+1)$ colours. Expressions for $K_1(\tau)$ and $K_2(\tau)$ in terms of infinite series are found for a generic function $\mathcal{F}(|i-j|)$ in the Gaussian orthogonal ensemble (GOE), the Gaussian unitary ensemble (GUE) and in the crossover between them (the almost unitary Gaussian ensemble). The Rosenzweig–Porter and power-law banded matrix ensembles are considered as examples.

PACS numbers: 71.23.−k, 71.23.An, 71.30.+h, 02.10.Yn

1. Introduction

Random matrix theory (RMT) has proved to be a universal formalism to describe a great variety of complex systems ranging from nuclei to mesoscopic quantum dots [1] to chaotic systems [2]. Of particularly wide application is the Wigner–Dyson RMT [3–5]. It is the statistical theory of eigenvalues and eigenfunctions of a random Hermitian matrix $\hat{H}$ whose entries $H_{i\geqslant j}$ fluctuate as independent Gaussian random variables with zero mean $\langle H_{ij}\rangle = 0$ and a constant variance $\langle|H_{ij}|^2\rangle = \text{const}$. There are three Dyson symmetry classes labelled by β: orthogonal ($\beta = 1$), unitary ($\beta = 2$) and symplectic ($\beta = 4$) that correspond to real, generic complex and real quaternionic Hermitian matrices. This theory is extremely successful

in describing the spectrum of complex nuclei and the statistics of various observable quantities in mesoscopic quantum dots [1, 6, 7].

The key property of the Wigner–Dyson RMT is that the variance $\langle|H_{ij}|^2\rangle$ does not change with increasing distance $|i-j|$ from the diagonal. In order to illustrate the properties of eigenvectors one can invoke a one-dimensional chain of sites $1 < i < N$ (N is the matrix size) with on-site energies H_{ii} and hopping matrix elements H_{ij}. Then the above property of off-diagonal entries implies the possibility of hopping throughout the entire chain which results in the delocalized character of eigenvectors. If on the contrary the off-diagonal matrix elements H_{ij} are non-zero only inside the band $|i-j| < \lambda$, all the eigenvectors turn out to be localized in the same way as in a quasi one-dimensional disordered wire [8]. This *banded random matrix* (BRM) theory is also relevant for chaotic systems under a time-periodic perturbation [2].

One well-known extension of the Wigner–Dyson RMT is the model of Rosenzweig and Porter [9] (RPRM) with the variance $\langle|H_{i\neq j}|^2\rangle = \mathcal{B}^2/N^{2\alpha}$ that does not depend on the distance $|i-j|$ but depends on the matrix size. The spectral statistics of RPRM at different parameters α can range from almost uncorrelated levels (if $\alpha > 1$) to a strong level repulsion which is similar to a weakly perturbed Wigner–Dyson ensemble (if $\alpha = 1/2$), see, for instance, the papers [11–13] and references therein. Exact calculation of the two-level correlation function of RPRM with the complex hopping entries $H_{i\neq j}$ and $\alpha = 1$ shows that the spectral statistics falls neither into the Poissonian nor into the Wigner–Dyson universality classes [10]. It is often called 'the regime of crossover'. Much less is known about RPRM with either real or quaternionic hopping elements [13].

Without loss of generality, RPRM can be presented by an ensemble of the matrices $\hat{H}_{RP} = \hat{A} + (\mathcal{B}/N^{\alpha})\hat{B}$ with a superposition of a diagonal matrix $\hat{A}$ and a full Wigner–Dyson matrix $\hat{B}$ of any symmetry ($\beta = 1, 2, 4$). If $\hat{A}$ is the random matrix possessing the Poissonian level statistics and $\mathcal{B} = 0$, the model describes spectral properties of a classical integrable system. By increasing $\mathcal{B}$ one can explore a transition from an integrable to a classically chaotic system with or without the time-reversal symmetry [12].

Recently another Gaussian RMT that interpolates between the Wigner–Dyson RMT and BRM theory attracted considerable attention. This is the *power-law banded random matrix* (PLBRM) theory [14–17] for which $\langle|H_{ij}|^2\rangle$ is nearly constant inside the band $|i-j| < \lambda$ and decreases as a power-law function $\langle|H_{ij}|^2\rangle \sim 1/|i-j|^{-2\alpha}$ for $|i-j| > \lambda$. The special case $\alpha = 1$ is relevant for the description of critical systems with multifractal eigenstates [14–19], in particular for systems at the Anderson localization–delocalization transition point. The case $\alpha > 1$ corresponds to the power-law localization which can be found in certain periodically driven quantum-mechanical systems [20].

The progress in BRM and PLBRM theories became possible because of mapping [8, 14] onto the non-linear supersymmetric sigma-model [21] that allowed us to obtain rigorous results by using various powerful methods of field theory. However, such mapping is only justified if the bandwidth $\lambda \gg 1$. In the opposite case where all the off-diagonal matrix elements are parametrically small compared to the diagonal ones, no field-theoretical approach is known so far. Yet such *almost diagonal* RMT may possess non-trivial properties because of the slow decay of the off-diagonal matrix elements $\langle|H_{ij}|^2\rangle$ with increasing $|i-j|$. For instance, it is of fundamental interest to study the spectral statistics in systems with *power-law localization* that takes place in the power-law banded random matrix ensembles at $\alpha > 1$. Another problem to study is the critical almost diagonal PLBRM. It is known that the eigenvectors of PLBRM with $\alpha = 1$ remain multifractal for an arbitrary small value of λ [19]. This means that the typical eigenfunction is *extended* though very sparse at small λ. Thus, almost diagonal random matrices may display the *localization–delocalization transition* by changing the

exponent α as well as their large bandwidth counterpart [14]. This transition has been studied numerically [22] for $\lambda \sim 1$ but little is known about it in the limit of almost diagonal random matrices.

The goal of this paper is to develop a formalism that would allow us to describe the spectral statistics for a *wide class of almost diagonal random matrices* with a generic behaviour of $\langle |H_{i\neq j}|^2 \rangle = b^2 \mathcal{F}(|i-j|)$ and $\langle |H_{ii}|^2 \rangle \sim 1$. The parameter b may or may not depend on the matrix size N. The principal requirement is that $b \ll 1$ is *small*. It controls the smallness of the off-diagonal matrix elements and will be used as an expansion parameter for the spectral correlation functions.

A natural way to proceed with such an expansion is to develop a perturbation theory in the parameter b starting from the diagonal matrix as a zero-order approximation. However, a naive expansion of the spectral form-factor $K(\tau)$ up to a finite order in b may fail, since the parameter b enters the product $bN\tau$ with the matrix size N and the time τ measured in units of the Heisenberg time. In this combination, the small parameter b can be compensated by the (large) product $N\tau$. In order to be able to obtain the *regular expansion in powers of* b, $K(\tau) = 1 + bK_1(\tau) + b^2K_2(\tau) + \cdots$, in the thermodynamic limit $N \to \infty$ at arbitrary $N\tau$, we develop a diagrammatic technique that gives $K_m(\tau)$ in a form of *infinite series* in powers of $bN\tau$. It is essentially a kind of locator expansion [23] adjusted to the problem of spectral statistics. It formalizes and generalizes the idea of [19] where the resonance pairs of states i, j with $|H_{ii} - H_{jj}| < |H_{ij}|$ have been considered to find the statistics of multifractal eigenstates. In our approach, the coefficients $K_m(\tau)$ result from an interaction (via the off-diagonal elements H_{ij}) of $m+1$ energy levels. We call this expansion a *virial expansion* by analogy with the expansion of thermodynamic functions of a dilute system in powers of density with *virial coefficients* that take into account collisions of $m+1$ particles. We stress that what we are doing below is not an *approximation* of two, three or more *resonant* levels. It is rather the *classification* of exact perturbation series by a number of the interacting levels involved. The question of a contribution from non-resonant levels does not arise, since at a given number of the interacting levels all possible relations between $|H_{ii} - H_{jj}|$ and $|H_{ij}|$ are taken into account.

The most serious problems on that route are (i) dealing with non-commutative matrices $\hat{H}_\varepsilon = \mathrm{diag}\{H_{ii}\}$ and $\hat{V} = \hat{H} - \hat{H}_\varepsilon$; (ii) combinatorial coefficients in the infinite series in $bN\tau$. The first problem is solved by using the *Trotter formula* (see section 3). The second problem reduces to a particular case of the general problem of graph colouring that is amenable to an exact solution (see sections 4 and 5).

As a result, we present the series for $K_m(\tau)$ with combinatorial coefficients that do not depend on the particular choice of $\mathcal{F}(|i-j|)$ in the variance $\langle |H_{ij}|^2 \rangle = b^2\mathcal{F}(|i-j|)$. They can thus be applied to *any* Gaussian ensemble of almost diagonal random matrices. Particularly simple expressions are found for $m = 1, 2$ which correspond to two and three interacting levels.

The general formulae obtained in this way are illustrated in section 7.1 for RPRM with $b = \mathcal{B}/N$; $\mathcal{F}(|i-j|) = 1$ and in section 7.2 for a critical PLBRM with $b = \mathcal{B}$; $\mathcal{F}(|i-j|) \sim 1/|i-j|^2$. In both examples, the constant $\mathcal{B}$ will be taken small: $\mathcal{B} \ll 1$. As a result, the correction to the Poisson behaviour $K(\tau) = 1$ has been obtained in the limit of infinite matrix size $N \to \infty$. The existence of such a correction can be interpreted as a rigorous detection of *delocalization* in the framework of a formalism that starts from the diagonal random matrix where all states are *localized*. Thus, our theory offers a *controllable way of obtaining delocalization from localization*. This is just complementary to conventional approaches based on the supersymmetric sigma-model [21] that always starts from delocalized (e.g., diffusive) modes.

2. Basic definitions

Let us consider a Hermitian RM of size $N \times N$, $N \gg 1$, from a Gaussian ensemble. We assume that entries of the matrix are random and independent. The RM is the Hamiltonian $\hat{H}$ of the matrix Schrödinger equation

$$\hat{H}\psi_n = \epsilon_n \psi_n$$

where ϵ_n and ψ_n are the eigenvalues and eigenvectors, respectively. Define statistical properties of the matrix entries:

$$\langle H_{i,j} \rangle = 0 \qquad \left\langle H_{i,i}^2 \right\rangle = \frac{1}{\beta} \qquad \langle |H_{i\neq j}|^2 \rangle = b^2 \mathcal{F}(|i-j|) \tag{1}$$

where $\mathcal{F}(|i-j|) > 0$ is a smooth function of its argument, and the parameter b is small:

$$b \ll 1.$$

The condition $b \ll 1$ means that RM is *almost diagonal*. The parameter β corresponds to the Dyson symmetry classes: $\beta_{\mathrm{GOE}} = 1$, $\beta_{\mathrm{GUE}} = 2$. The brackets $\langle \cdots \rangle$ denote the ensemble averaging. If the ensemble is Gaussian the averaging of a function $F(A)$ over a random variable A reads

$$\langle F(A) \rangle_A \equiv \frac{1}{\sqrt{2\pi \bar{A}^2}} \int_{-\infty}^{+\infty} F(A) \exp\left(-\frac{A^2}{2\bar{A}^2}\right) \mathrm{d}A.$$

We concentrate on the level statistics which is characterized by the density of states $\rho(E) = \sum_n \delta(E - \epsilon_n)$ and its multi-point correlation functions. For example, the two-level correlation function $R(\omega)$ is defined as

$$R(\omega) = \frac{\langle\langle \rho(\omega/2)\rho(-\omega/2) \rangle\rangle}{\langle \rho(0) \rangle^2} \qquad \langle\langle \hat{a}\hat{b} \rangle\rangle \equiv \langle \hat{a}\hat{b} \rangle - \langle \hat{a} \rangle \langle \hat{b} \rangle. \tag{2}$$

The Fourier transform of $R(\omega)$ is known as the spectral form-factor $K(t)$:

$$K(t) = \int_{-\infty}^{+\infty} \mathrm{e}^{\mathrm{i}\omega t} R(\omega)\, \mathrm{d}\omega. \tag{3}$$

We will see below that for almost diagonal RM the representation of spectral statistics in the time domain turns out to be convenient. Therefore, from now on we use the form-factor instead of the correlation function. We rescale time by the mean level spacing $\Delta \equiv 1/\langle \rho(0) \rangle$ introducing the dimensionless time $\tau = t\Delta$. Our goal is to develop a regular perturbative expansion for $K(\tau)$ in powers of small parameter $b \ll 1$. In the limit of small time the spectral form-factor $K(\tau \to 0)$ is linked to the other important spectral characteristics called *the level compressibility* [24]:

$$\chi = \lim_{\tau \to 0} \left(\lim_{N \to \infty} K(\tau) \right). \tag{4}$$

Let us take a window of the width δE, $\delta E/\Delta \equiv \bar{n} \ll N$, in the energy space centred at $E = 0$ and calculate the number n of levels inside the window at some realization of disorder. The level number variance is $\Sigma_2(\bar{n}) = \langle (n - \bar{n})^2 \rangle$. The level compressibility is by definition the limit

$$\chi = \lim_{\bar{n} \to \infty} \left(\lim_{N \to \infty} \frac{\partial \Sigma_2(\bar{n})}{\partial \bar{n}} \right). \tag{5}$$

The level compressibility contains information about the localization transition: χ ranges from $\chi_{\mathrm{WD}} = 0$ for the Wigner–Dyson statistics with extended wavefunctions and a strong level repulsion to $\chi_P = 1$ in the case of localized wavefunctions and uncorrelated levels with

the Poissonian distribution. The intermediate situation with $0 < \chi_{\rm crit} < 1$ is inherent for the critical regime of multifractal wavefunctions [24].

The main object of our further analysis is the following correlation function in the time domain:

$$\tilde{K}_N(\tau) = \frac{1}{N}\langle\langle \mathrm{Tr}\, \mathrm{e}^{-\mathrm{i}\hat{H}\tau/\Delta}\, \mathrm{Tr}\, \mathrm{e}^{\mathrm{i}\hat{H}\tau/\Delta}\rangle\rangle \equiv \tilde{K}_0(\tau) + b\tilde{K}_1(\tau) + b^2\tilde{K}_2(\tau) + \cdots. \tag{6}$$

For the constant mean density of states $\tilde{K}(\tau)$ coincides with $K(\tau)$. However, they are different if $\langle\rho(E)\rangle$ essentially depends on energy E. In analogy with equation (4) one can define the quantity $\chi_0 \equiv \lim_{\tau\to 0}(\lim_{N\to\infty}\tilde{K}_N(\tau))$. It turns out that at small b there is a simple approximate relationship between χ and χ_0 (see appendix A):

$$\chi \simeq 1 - \frac{1-\chi_0}{\Upsilon} \qquad \Upsilon = \frac{\Delta}{N}\int_{-\infty}^{+\infty}\langle\rho(E)\rangle^2\,\mathrm{d}E. \tag{7}$$

The mean density of states for the Gaussian ensemble of almost diagonal RMs with either localized or (sparse) fractal eigenstates is close to the Gaussian distribution of the diagonal entries [25]:

$$\langle\rho(E)\rangle \simeq N\sqrt{\frac{\beta}{2\pi}}\exp\left(-\frac{\beta E^2}{2}\right) \Rightarrow \Delta \simeq \frac{1}{N}\sqrt{\frac{2\pi}{\beta}}. \tag{8}$$

Thus, with an accuracy of $O(b)$ the unfolding factor in equation (7) can be taken as $\Upsilon^{-1} \simeq \sqrt{2}$.

3. The method

3.1. The Trotter formula

As far as we investigate the properties of almost diagonal RMs, the Hamiltonian can be naturally divided into a diagonal part $\hat{H}_\varepsilon$ and a matrix of hopping elements $\hat{V}$:

$$\hat{H} \equiv \hat{H}_\varepsilon + \hat{V}. \tag{9}$$

It follows from definition (1) that the hopping elements $H_{i,j} \equiv V_{i,j} \sim b$ are small compared to the diagonal ones $H_{i,i} \equiv \varepsilon_i \sim 1$. However, matrices $\hat{H}_\varepsilon$ and $\hat{V}$ do not commute with each other and a direct expansion of the exponentials $\mathrm{e}^{\pm\mathrm{i}(\hat{H}_\varepsilon+\hat{V})\frac{\tau}{\Delta}}$ in equation (6) in terms of $\hat{V}$ involves serious difficulties. One possible way to overcome these problems is to represent $\mathrm{e}^{\pm\mathrm{i}(\hat{H}_\varepsilon+\hat{V})\frac{\tau}{\Delta}}$ as a product of exponential functions containing matrices $\hat{H}_\varepsilon$ and $\hat{V}$ separately. To do this we use a generalization of the identity $\exp(a+b) \equiv \exp(a)\exp(b)$ for non-commuting variables known as the *the Trotter formula* [26]:

$$\mathrm{e}^{\hat{A}+\hat{B}} = \lim_{n\to\infty}(\mathrm{e}^{\hat{A}/n}\,\mathrm{e}^{\hat{B}/n})^n \quad \Rightarrow \quad \mathrm{e}^{\pm\mathrm{i}\hat{H}\frac{\tau}{\Delta}} = \lim_{n\to\infty}\prod_{p=1}^{n}(\mathrm{e}^{\pm\mathrm{i}\hat{H}_\varepsilon\frac{\tau}{\Delta n}}\,\mathrm{e}^{\pm\mathrm{i}\hat{V}\frac{\tau}{\Delta n}}). \tag{10}$$

The Trotter formula is exact for the finite matrices $\hat{A}$ and $\hat{B}$. Therefore, the correct order of limits reads

$$\begin{array}{ll} 1 & n\to\infty \\ 2 & N\to\infty \\ 3 & \text{(if necessary) } \tau\to 0. \end{array} \tag{11}$$

In what follows we will always imply precisely this order of doing limits.

Equation (10) allows us to make a regular expansion in powers of $\hat{V}$. The price for that is the infinite product in equation (10). We need a proper selection rule to extract from that product terms of the order of $O(b^0)$, $O(b^1)$, $O(b^2)$, ...

3.2. Lowest-order terms

For a strictly diagonal matrix the spectral form-factor $\tilde{K}(\tau)$ is calculated straightforwardly:

$$\tilde{K}(\tau)|_{\hat{V}=0} = \frac{1}{N}\langle\langle \mathrm{Tr}\, \mathrm{e}^{-\mathrm{i}\hat{H}_\varepsilon \tau/\Delta}\, \mathrm{Tr}\, \mathrm{e}^{\mathrm{i}\hat{H}_\varepsilon \tau/\Delta}\rangle\rangle = \frac{1}{N}\sum_l [1 - \langle \mathrm{e}^{-\mathrm{i}\varepsilon_l \tau/\Delta}\rangle^2] = 1 - \mathrm{e}^{-\langle\varepsilon^2\rangle(\tau/\Delta)^2}. \quad (12)$$

For all Gaussian RM of the type equation (1) the inverse mean level spacing increases with the matrix size N. The inverse mean level spacing $1/\Delta \equiv \tilde{N}$ is proportional to the matrix size: $\tilde{N} \sim N$. For finite N the normalization sum rule [24] requires $\tilde{K}(0) = 0$. If, however, the limit $N \to \infty$ is done *prior* to the limit $\tau \to 0$ (see equation (11)) the normalization sum rule is violated and we recover the Poisson statistics result $\tilde{K}(\tau) = 1$.

In order to obtain corrections to $\tilde{K}(\tau)$ proportional to b^k one has to expand $\mathrm{e}^{\pm\mathrm{i}\tilde{N}\tau\hat{V}/n}$ in powers of $\hat{V}$ in the infinite product in the r.h.s. of equation (10):

$$\underbrace{\cdots \times \exp\left(\pm\mathrm{i}\tfrac{\tilde{N}\tau}{n}\hat{H}_\varepsilon\right)\exp\left(\pm\mathrm{i}\tfrac{\tilde{N}\tau}{n}\hat{V}\right) \times \exp\left(\pm\mathrm{i}\tfrac{\tilde{N}\tau}{n}\hat{H}_\varepsilon\right)\exp\left(\pm\mathrm{i}\tfrac{\tilde{N}\tau}{n}\hat{V}\right) \times \cdots}_{n \text{ pairs of exponentials}} \quad (13)$$

and then to perform the Gaussian averaging over $\hat{H}_\varepsilon$ and $\hat{V}$. Note that the Gaussian average is zero for all terms on the r.h.s of equation (6) which contain an odd number of off-diagonal matrices $\hat{V}$. That is why only terms with *even* powers of b may result from such an expansion. For the purpose of explaining the details of the new formalism based on the Trotter formula we show how the term $\propto b^2$ arises from it.

3.2.1. Gaussian averaging. Each $\mathrm{Tr}\, \mathrm{e}^{\pm\mathrm{i}H\tilde{N}\tau}$ in equation (6) can be represented using the Trotter formula as Tr of the infinite product equation (13). Therefore, we have to expand either *two* exponentials $\mathrm{e}^{\pm\mathrm{i}\hat{V}\tilde{N}\tau/n}$ in equation (13) up to $\hat{V}$ or one single exponential up to $\hat{V}^2$ setting $\hat{V} = 0$ in all the other exponentials $\mathrm{e}^{\pm\mathrm{i}\hat{V}\tilde{N}\tau/n}$. We will show below that only the first option survives the limit $n \to \infty$.

Expanding two of $\exp\left(\pm\mathrm{i}\frac{\tilde{N}\tau}{n}\hat{V}\right)$ in equation (13) up to $\hat{V}^1$ we obtain[3]:

$$\exp\left(\pm\mathrm{i}\frac{\tilde{N}\tau p_1}{n}\hat{H}_\varepsilon\right)\left(\pm\mathrm{i}\frac{\tilde{N}\tau}{n}\hat{V}\right)\exp\left(\pm\mathrm{i}\frac{\tilde{N}\tau p_2}{n}\hat{H}_\varepsilon\right)\left(\pm\mathrm{i}\frac{\tilde{N}\tau}{n}\hat{V}\right)\exp\left(\pm\mathrm{i}\frac{\tilde{N}\tau p_3}{n}\hat{H}_\varepsilon\right) \sim b^2 \quad (14)$$

where $p_{1,2,3}$ are the numbers of successive exponentials $\exp\left(\pm\mathrm{i}\frac{\tilde{N}\tau}{n}\hat{H}_\varepsilon\right)$ 'fused' together after we set $\hat{V} = 0$ in all $\exp\left(\pm\mathrm{i}\frac{\tilde{N}\tau}{n}\hat{V}\right)$ but two. We call p_s *the Trotter numbers*. They obey the obvious restriction

$$p_1 + p_2 + p_3 = n \qquad p_{1,2} \geqslant 1 \qquad p_3 \geqslant 0. \quad (15)$$

Note that both off-diagonal matrices $\hat{V}$ in equation (14) must belong to the same trace. If they belong to the different traces the result is zero because $\mathrm{Tr}\left\{\exp\left(\pm\mathrm{i}\frac{\tilde{N}\tau p_i}{n}\hat{H}_\varepsilon\right)\hat{V}\right\} = 0$.

[3] The expression $\exp(-\mathrm{i}\frac{\tilde{N}\tau}{n}\hat{H}_\varepsilon)$ can be compared with a locator in the locator expansion while $\exp(-\mathrm{i}\frac{\tilde{N}\tau}{n}\hat{V})$ produces interactors [23].

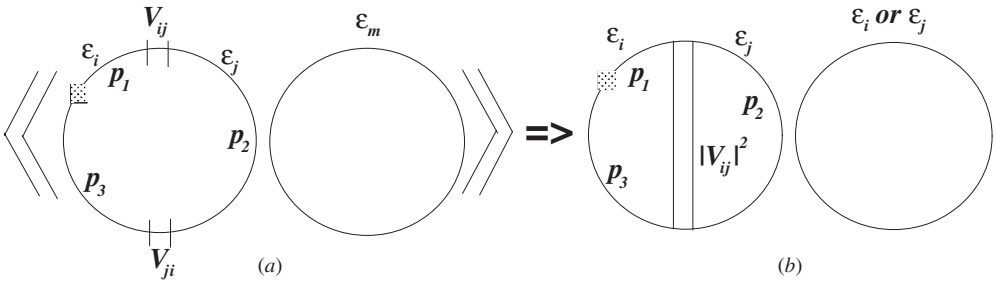

Figure 1. Graphic illustration of equation (16) before (*a*) and after (*b*) averaging.

In order to find the term $\mathcal{C} \propto O(b^2)$ in equation (6) we substitute equation (14) into equation (6) and perform the Gaussian averaging in accordance with equation (1):

$$\mathcal{C} = -\frac{4}{N}\left(\frac{\tilde{N}\tau}{n}\right)^2 \sum_{\{p_s\}}^{n} \left\langle\!\!\left\langle \sum_{i,j,m=1}^{N} \mathrm{e}^{-\mathrm{i}\frac{\tilde{N}\tau p_1}{n}\varepsilon_i} V_{i,j}\, \mathrm{e}^{-\mathrm{i}\frac{\tilde{N}\tau p_2}{n}\varepsilon_j} V_{j,i}\, \mathrm{e}^{-\mathrm{i}\frac{\tilde{N}\tau p_3}{n}\varepsilon_i} \times \mathrm{e}^{\mathrm{i}\tilde{N}\tau\varepsilon_m} \right\rangle\!\!\right\rangle \Bigg|_{m=i \text{ or } m=j}$$
$$= -4\frac{(b\tilde{N}\tau)^2}{n^2}\mathcal{R}_N(1) \sum_{\{p_s\}}^{n} \left\{ \mathcal{D}_N\Big(\frac{n-p_1-p_3}{n}\Big)\mathcal{D}_N\Big(\frac{p_2}{n}\Big) + \mathcal{D}_N\Big(\frac{p_1+p_3}{n}\Big)\mathcal{D}_N\Big(\frac{n-p_2}{n}\Big) \right\} \tag{16}$$

where $\sum_{\{p_s\}}^{n}$ means summation over the Trotter numbers $\sum_{p_1,p_2,p_3=1}^{n}\delta_{n-(p_1+p_2+p_3)}$ and we denote

$$\mathcal{D}_N(y) \equiv \exp\left[-\frac{1}{2\beta}(\tilde{N}\tau)^2 y^2\right] \qquad \mathcal{R}_N(k) \equiv \frac{1}{N}\sum_{i>j}^{N}(\mathcal{F}(|i-j|))^k. \tag{17}$$

The function $\mathcal{R}_N(k)$ depends on the particular form of decay of the off-diagonal matrix elements in the Gaussian ensemble (see equation (1)) and contains the sum over matrix indices which will be below referred to as the summation over the 'real space'.

It is instructive to give a graphic representation of equation (16) before and after averaging. In figure 1 each circle denotes the trace. The vertices $V_{i,j}$ and $V_{j,i}$ in the left circle are uncoupled before averaging (figure 1(*a*)). The shadowed box indicates the starting point of the Trotter chain equation (13). The circle is thus divided into segments (below referred to as the *Trotter segments*) corresponding to $\mathrm{e}^{-\mathrm{i}\frac{\tilde{N}\tau p_1}{n}\varepsilon_i}$, $\mathrm{e}^{-\mathrm{i}\frac{\tilde{N}\tau p_2}{n}\varepsilon_j}$ and $\mathrm{e}^{-\mathrm{i}\frac{\tilde{N}\tau p_3}{n}\varepsilon_i}$. We mark the length of each segment by the Trotter number p_s. The right circle stands for $\mathrm{e}^{\mathrm{i}\tilde{N}\tau\varepsilon_m}$. The averaging over $\hat{V}$ connects uncoupled V-vertices by the correlation function $|V_{ij}|^2 = b^2\mathcal{F}(|i-j|)$ denoted by a double line while the averaging over ε_m couples ε_m to either ε_i or ε_j (figure 1(*b*)).

3.2.2. Integral over Trotter variables. One has to sum over the Trotter numbers in equation (16) prior to taking the limit $n \to \infty$. To this end we introduce the *Trotter variables* $y_s = p_s/n$ which in the limit $n \to \infty$ can be considered as continuous. Then the summation over the Trotter numbers p_s can be replaced by integration over the Trotter variables. Switching

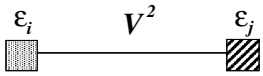

Figure 2. Graphic illustration of the simplest term $\mathcal{C}$.

from the Kronecker-delta δ_p to the Dirac δ-function $n\delta_p \to \delta(y)$ we arrive at

$$\mathcal{C} = -4(b\tilde{N}\tau)^2\mathcal{R}_N(1)\mathcal{I}$$

$$\mathcal{I} = \iiint_0^1 \mathrm{d}y_1\,\mathrm{d}y_2\,\mathrm{d}y_3\,\delta(1-y_1-y_2-y_3)\{\mathcal{D}_N(1-y_1-y_3)\,\mathcal{D}_N(y_2) + \mathcal{D}_N(y_1+y_3)\,\mathcal{D}_N(1-y_2)\}. \tag{18}$$

It is remarkable that as a result of this transformation, which is exact in the $n \to \infty$ limit, all the n-dependent factors are absorbed by y_s. This is because the number of independent Trotter numbers p_s in equation (16) coincides with the number of matrices $\hat{V}$, each coming with the factor $1/n$. Note that this is not the case if only one exponential $\mathrm{e}^{\pm\mathrm{i}\hat{V}\tilde{N}\tau/n}$ in equation (13) is expanded up to $\hat{V}^2$ order. Then the number of Trotter summations is less by one which leaves an uncompensated factor $1/n \to 0$ after switching to the Trotter variables. Thus, we arrive at an important conclusion that *in all orders* of $\hat{V}$-expansion one should retain only *linear* terms of expansion of the exponential $\mathrm{e}^{\pm\mathrm{i}\hat{V}\tilde{N}\tau/n} \approx 1 \pm \mathrm{i}\hat{V}\tilde{N}\tau/n$.[4]

The integral equation (18), which will be referred to as 'the Trotter integral', can be simplified by observing that the δ-function imposes the same arguments in both $\mathcal{D}_N$ functions in the corresponding products. Thus $\mathcal{D}_N$ functions can be fused $\mathcal{D}_N(x)\mathcal{D}_N(x) \equiv \mathcal{D}_N(\sqrt{2}x)$ and the Trotter integral takes the form:

$$\mathcal{I} = \int_0^1 \mathrm{d}y(1-y)\{\mathcal{D}_N(\sqrt{2}y) + \mathcal{D}_N(\sqrt{2}[1-y])\}. \tag{19}$$

A similar fusion takes place in the Trotter integrals at an arbitrary order of V-expansion.

Further simplification is possible only in taking the thermodynamic limit $N \to \infty$. In this limit the function $\mathcal{D}_N(y)$ defined in equation (17) collapses to the δ-function:

$$\mathcal{D}_N(\sqrt{2}y)|_{N\to\infty} \simeq \frac{\sqrt{\pi\beta}}{\tilde{N}|\tau|}\delta(y). \tag{20}$$

Then integral (19) is easily calculated and we find finally the expression for $\mathcal{C}$:

$$\mathcal{C} = -b\sqrt{\beta\pi}(b\tilde{N}|\tau|)\,\mathcal{R}_N(1) \tag{21}$$

where $\mathcal{R}_N(1)$ is given by equation (17).

Let us look at the calculation of $\mathcal{C}$ from a different viewpoint. Namely, we note that in this calculation only two species of levels i and j are involved. We show this situation graphically in figure 2. Shadowed boxes mark the energy levels with different shadowing ('colours') for ε_i and ε_j. They are connected by the interaction line (IL) which is associated with the factor $(\tilde{N}\tau b)^2$. Because of the fusion of two $\mathcal{D}_N$-functions, the interaction of *two* levels brings only *one* δ-function with the normalization factor $1/(\tilde{N}|\tau|)$. As a result, we get one 'free' parameter b which is decoupled from the combination $\tilde{N}|\tau|$ that involves the matrix size N:

$$\mathcal{C} \sim \frac{(\tilde{N}\tau b)^2}{\tilde{N}|\tau|}\mathcal{R}_N(1) = b^1 \times (\tilde{N}|\tau|b)^1\mathcal{R}_N(1).$$

It is clear from the above analysis that if we continue expanding in higher powers of $V_{ij} = V_{ji}^*$ but keep the number of colours equal to 2, we will increase the power of the combination $(b\tilde{N}|\tau|)$ but not the power of the free parameter b.

[4] This is similar to a derivation of path integrals technique with the help of the Trotter formula, see, for instance [27].

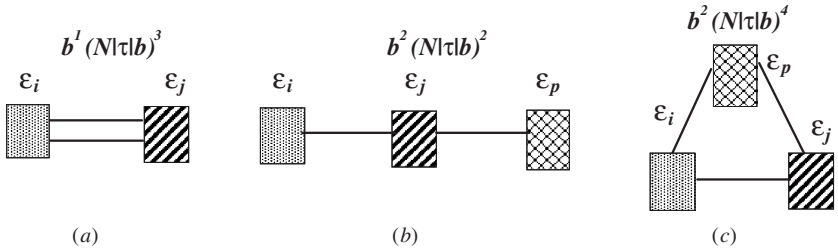

Figure 3. Example of diagrams classified in accordance with the selection rule: (*a*) the case of two colours: $k = k_1 = 2$; (*b*) and (*c*) two simplest diagrams for the case of three colours: (*b*) $k = 2, k_1 = 1, k_2 = 1$ and (*c*): $k = 3, k_1 = 1, k_2 = 1, k_3 = 1$.

3.3. Selection rule

Consider a generic term of order b^{2k} in the perturbation series:

$$\mathcal{C}_{2k}(\mathsf{A},\mathsf{B}) = C_N(\{k_i\})\, b^{\mathsf{A}}(\tilde{N}|\tau|b)^{\mathsf{B}} \qquad \mathsf{A}+\mathsf{B} \equiv 2k. \tag{22}$$

It corresponds to a diagram with $k = k_1 + k_2 + \cdots$ interaction lines distributed in a certain way $\{k_i\} = \{k_1, k_2, \cdots\}$ among the links connecting a given number of different energy levels ('*colours*').

Let us formulate the selection rule for such a perturbation theory.

- The power A of the 'free' parameter b is equal to the number of interacting energy levels minus 1: $\mathsf{A} = c - 1$.
- The sum $\mathsf{A}+\mathsf{B}$ is equal to $2k$.

We exemplify it in figure 3 for three different diagrams: the diagram with two colours (*a*) corresponding to $k = 2, \mathsf{A} = 1, \mathsf{B} = 3$; and two diagrams with three colours: (*b*) for $k = 2, \mathsf{A} = 2, \mathsf{B} = 2$ and (*c*) for $k = 3, \mathsf{A} = 2, \mathsf{B} = 4$.

Suppose that we want to derive the perturbative term $\tilde{K}_{\mathsf{A}}(\tau)$ of the order of $O(b^{\mathsf{A}})$, which would be valid at an arbitrary value of $\tilde{N}|\tau|b$ in the limit $N \to \infty$. Such a physical result can be obtained using the following strategy:

(1) Fix the power A of the 'free' small parameter b by fixing the number of interacting energy levels, i.e. the number of colours: c.
(2) Perform summation of an infinite series in $\tilde{N}|\tau|b$ at fixed c over the number(s) k_i of IL along each link.
(3) Analyse the limit $N \to \infty$ of the corresponding *infinite* series in $\tilde{N}|\tau|b$.

If this virial expansion works the series should converge in the limit $N \to \infty$.

The strategy we suggested is a certain way of summation of perturbative series. Its physical meaning is analogous to the idea of resonant energy levels [19] or locator expansion [23]. However, in contrast to these essentially heuristic approaches our selection rule offers a formalism that allows us to implement a regular expansion in the small parameter b. It takes into account resonant as well as non-resonant levels accurately which is impossible in the above heuristic methods.

Concluding this section we would like to note that the coefficient $C_N(\{k_i\})$ in equation (22) is a product of two different factors:

$$C_N(\{k_i\}) = \mathcal{R}_N(\{k_i\})\mathcal{V}(\{k_i\}) \tag{23}$$

where $\mathcal{V}(\{k_i\})$ is a universal coefficient which depends on a combinatorial factor $\mathcal{K}$ and on the corresponding Trotter integral $\mathcal{I}$. The factor $\mathcal{R}(\{k_i\})$ is not universal. It arises because of the

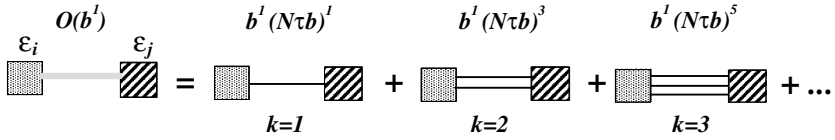

Figure 4. The two-colour diagrams.

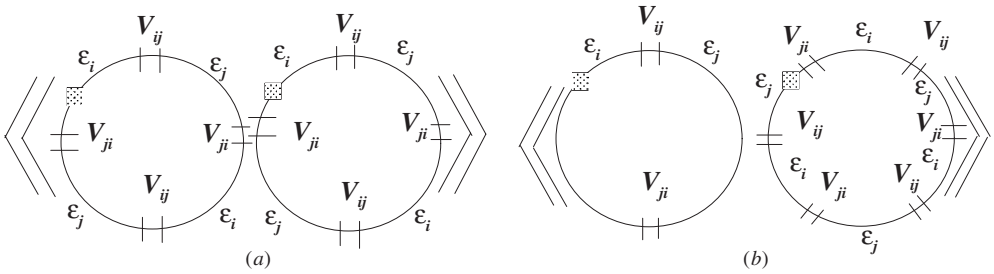

Figure 5. Two examples of different distributions of $\hat{V}$ at $k = 4$. The first segment of the Trotter chain is denoted by the shadowed box.

summation of the product of the correlation functions $\mathcal{F}(|i - j|)$ over the real space and is a generalization of the function $\mathcal{R}_N(k)$ given by equation (17). In the large-N limit it can be represented as

$$\mathcal{R}_N(\{k_i\}) = \mathcal{R}(\{k_i\}) + \frac{1}{N}\mathcal{R}^{(1)}(\{k_i\}) + \cdots \tag{24}$$

where $\mathcal{R}(\{k_i\})$ and $\mathcal{R}^{(1)}(\{k_i\})$ are of the same order. In this paper, we study mainly a contribution of the leading term $\mathcal{R}(\{k_i\})$. The role of the $1/N$ corrections to $\mathcal{R}(\{k_i\})$ is discussed in section 7.2.

4. The case of two colours

In this section we calculate the term of order b in $\tilde{K}(\tau)$. According to a general scheme outlined in the previous section this correction is governed by the two-colour diagrams (figure 4) which correspond to the following power series:

$$b\tilde{K}_1 = \sum_{k=1}^{\infty}(-1)^k x^{2k}\mathcal{V}(k)\mathcal{R}_N(k) \qquad \mathcal{V}(k) = \mathcal{K}(k)\mathcal{I}(k) \qquad x \equiv \tilde{N}|\tau|b. \tag{25}$$

The main difficulty in this calculation is the universal factor $\mathcal{V}(k)$ in equation (25). Applying the Trotter formula to both traces in equation (6) and making an expansion in $\hat{V}$ analogous to equation (14) we observe that the same number of IL may correspond to completely different distributions of the off-diagonal matrices $\hat{V}$ over two traces (see figure 5).

The combinatorial part of the calculation consists of two tasks. One of them is to distribute colours (denoting $\varepsilon_{i,j}$) over $2k$ segments. Since $\hat{V}$ is the off-diagonal matrix, the adjacent colours in each circle must be different. In general, this is a particular case of the famous combinatorial problem of graph colouring [28]. For the case of only two colours (ε_i and ε_j) considered in this section the problem is trivial: each circle must contain an even number of the segments while the first segment of the Trotter chain corresponds either to ε_i or to ε_j (see figure 6), so that only the factor of 4 arises from this colouring. The second

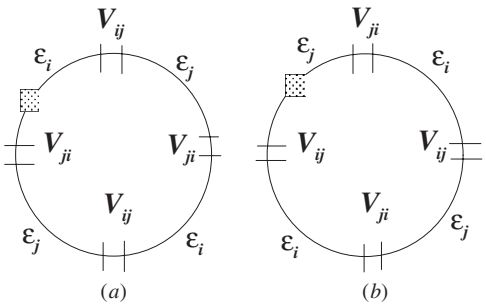

Figure 6. Two different ways to put colours in the two-colour problem. The first segment is denoted by the shadowed box.

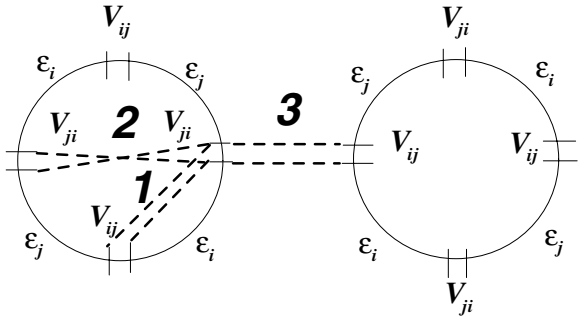

Figure 7. An example for three different connections of V-vertices at $k = 4$.

combinatorial task is to find the number of ways to connect V-matrices in pairs making either in-circle or inter-circle connections. Such connections are equivalent to Gaussian averaging.

In figure 7 we show three different ways to connect *two* V-matrices. Two links labelled by 1 and 2 are in-circle connections, while the third one (labelled by 3) is the inter-circle connection. The difference between the connections 1 and 2 is that the connection 1 corresponds to the average $\langle V_{ij}V_{ji}\rangle$ while the connection 2 corresponds to the average $\langle V_{ij}V_{ij}\rangle$. For *real* Hermitian matrices (the *orthogonal* ensemble, GOE, $\beta = 1$) $V_{ij} = V_{ji}$ both connections are possible and the corresponding averages are equal to each other. However, for *complex* Hermitian matrices with the same variance of the real and imaginary parts (the *unitary* ensemble, GUE, $\beta = 2$) only one of the two averages, $\langle V_{ij}V_{ji}\rangle$, is non-zero. In this case the 'crossed' connection 2 is not allowed.

Now one can easily find the combinatorial factors associated with the number of possible connections. In the GOE any of the $2k$ vertices V can be connected with any other V-vertex and we get

$$\mathcal{K}_{\mathrm{GOE}}(k) = 4 \times (2k-1)!!. \tag{26}$$

In the GUE the $2k$ V-vertices are divided by two groups: one group containing k vertices of V_{ij} and another group containing k vertices V_{ji}. The connection is possible only if V-vertices belong to *different* groups. Thus, we obtain for the corresponding combinatorial factor:

$$\mathcal{K}_{\mathrm{GUE}}(k) = 4 \times k!. \tag{27}$$

In order to find the coefficient $\mathcal{I}(k)$ we have to fix the number of $\hat{V}$ matrices in each trace to be $2m$ and $2(k-m)$, thereby also fixing the number of segments in the circles. Each segment

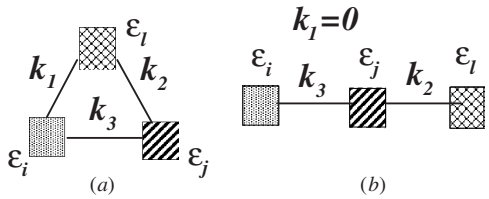

Figure 8. The three-colour diagrams: (*a*) a triangle diagram with $k_{1,2,3} > 0$; (*b*) a line diagram with $k_{2,3} > 0$ and $k_1 = 0$.

corresponds to a Trotter variable to be integrated over. The details of the calculation of the Trotter integral $\mathcal{I}(k)$ are presented in appendix B. The final result is obtained after summation over m:

$$\mathcal{I}(k) = b\frac{1}{\tilde{N}|\tau|b}\frac{\sqrt{\beta\pi}}{2}\frac{1}{k!(k-1)!}. \tag{28}$$

Substituting the combinatorial factor $\mathcal{K}(k)$, equations (26) and (27), and the Trotter integral (28) into the series (25) we find

$$\tilde{K}_1 = 2\sqrt{\pi\beta}\sum_{k=1}^{\infty}(-1)^k C_\beta^{(2)}(k)\mathcal{R}_N(k)(\tilde{N}|\tau|b)^{2k-1} \tag{29}$$

$$C_{\beta=1}^{(2)}(k) = \frac{(2k-1)!!}{k!(k-1)!} \tag{30}$$

$$C_{\beta=2}^{(2)}(k) = \frac{1}{(k-1)!}. \tag{31}$$

Equations (29)–(31) correspond to the leading in $b \ll 1$ correction to the Poisson spectral form-factor. They have been obtained in the framework of the two colour approximation when we have taken into account only pairs of the interacting energy levels. We note that the transformation (20) of the $\mathcal{D}_N$-function into the delta-function is approximate and its sub-leading terms yield the corrections to $b\tilde{K}_1$ of higher orders starting from $\sim b^3(\Delta\tilde{K}_1)$.

We emphasize formula (29) for $\tilde{K}_1$ is valid for a Gaussian random matrix ensemble with a generic variance of the off-diagonal matrix elements $\langle|V_{ij}|^2\rangle = b^2\mathcal{F}(|i-j|)$.

5. The case of three colours

According to the selection rule explained above, the term of order b^2 in $\tilde{K}(\tau)$ results from an interaction of three energy levels, i.e. we have to perform a summation of the three-colour diagrams, see figure 8. Three shadowed boxes stand for the three independent energy levels ε_i, ε_j and ε_l $(l > j > i)$, which are connected by ILs. Any two levels can be connected with each other independently of a connection with the third one by an arbitrary number of ILs: k_1, k_2 and k_3. This leads to a three-dimensional power series in $x = \tilde{N}|\tau|b$:

$$b^2\tilde{K}_2 = \sum_{k_{1,2,3}}^{\infty}(\mathrm{i}x)^{2(k_1+k_2+k_3)}\mathcal{V}(\{k_i\})\mathcal{R}_N(\{k_i\}) \qquad i = 1, 2, 3. \tag{32}$$

Here, the universal factor $\mathcal{V}(\{k_i\})$ contains the Trotter integral $\mathcal{I}(\{k_i\})$ and the combinatorial factor $\mathcal{K}(\{k_i\})$. The function $\mathcal{R}_N$ is a generalization of the sum in real space for the case of three colours:

$$\mathcal{R}_N(\{k_i\}) = \frac{1}{N}\sum_{l=j+1}^{N}\sum_{j=i+1}^{N}\sum_{i=1}^{N}[(\mathcal{F}(|i-j|))^{k_1}(\mathcal{F}(|j-l|))^{k_2}(\mathcal{F}(|l-i|))^{k_3}]. \tag{33}$$

Generically, any energy level interacts with the two others and all numbers of ILs are not zero $k_{1,2,3} > 0$. A diagram describing this case will be referred to as *a triangle* (see figure 8(*a*)). However, there are configurations where two levels do not interact with each other and one parameter k_i is zero. A corresponding diagram will be named *a line* (see figure 8(*b*)). We can attribute a certain physical meaning to both of the three-colour diagrams. Let us involve a tree-like structure in the real space where a path with loops is prohibited. It will generate only the 'lines'. In contrast, a real space structure where the paths with loops are allowed will yield both the 'triangles' and the 'lines'.

The combinatorial factor $\mathcal{K}$ includes the number of colouring of segments by three colours (denoting $\varepsilon_{i,j,l}$) and the number of ways to pair V-matrices by in-circle and inter-circle connections. The V-matrices create three sets of vertices in the circles: $2k_1$ vertices of $\{V_{i,l}, V_{l,i}\}$, $2k_2$ vertices of $\{V_{j,l}, V_{l,j}\}$ and $2k_3$ vertices of $\{V_{i,j}, V_{j,i}\}$. In view of the property

$$\langle V_{s,p}V_{q,r}\rangle = \left\langle V_{s,p}^2\right\rangle\delta_{s,q}\delta_{p,r} + \langle|V_{s,p}|^2\rangle\delta_{s,r}\delta_{p,q} \tag{34}$$

the vertices belonging to one and the same set must be paired with each other independent of the two other sets. Applying the same arguments that were used in the case of two colours we arrive at

$$\mathcal{K}_{\mathrm{GOE}} = \mathrm{Col}_{\mathrm{GOE}}\prod_{i=1,2,3}(2k_i-1)!! \tag{35}$$

$$\mathcal{K}_{\mathrm{GUE}} = \mathrm{Col}_{\mathrm{GUE}}\prod_{i=1,2,3}(k_i)! \tag{36}$$

where Col is the colouring factor. When the number of colours is larger than two the colouring factor is different in GOE and GUE. Details of calculation of Col are given in appendix C. Here we explain notation and give the results for GOE and GUE.

Denote the total number of segments for each of the three colours by R, G and B. These numbers can be expressed in terms of $k_{1,2,3}$:

$$R = k_1 + k_2 \qquad G = k_2 + k_3 \qquad B = k_3 + k_1.$$

The coloured segments are distributed over the two circles. The numbers of coloured segments in the first circle will be labelled r, g and b. Thus, the second circle contains $R-r$, $G-g$ and $B-b$ segments of different colours.

In the case of GOE, the two circles are coloured independently under the only condition that any two neighbouring segments must be of different colours (see appendix C). The factor $\mathrm{Col}_{\mathrm{GOE}}$ reads

$$\mathrm{Col}_{\mathrm{GOE}} = \mathrm{Col}^{(3)}(r,g,b)\times\mathrm{Col}^{(3)}(R-r,G-g,B-b)$$

$$\mathrm{Col}^{(3)}(a,b,c) \equiv (a+b+c)2^{a+b+c}\sum_{k=\max(a,b,c)}^{\frac{a+b+c}{2}}\frac{2^{-2k}(k-1)!}{(k-a)!(k-b)!(k-c)!(a+b+c-2k)!}. \tag{37}$$

Before exploring the case of GUE, we recall that the 'crossed' connections (see example 2 in figure 7) are not allowed in GUE. The 'crossed' connections can be avoided if each set of vertices $\{V_{p,q}, V_{q,p}\}$ contains exactly k_i $V_{p,q}$ vertices and k_i $V_{q,p}$ vertices regardless

to their distribution over the circles. Note, that this restriction applies only to the total number of $V_{p,q}$ and $V_{q,p}$ while the number of vertices $V_{p,q}$ and $V_{q,p}$ in the same circle is not necessarily balanced. The colouring of the two circles is no longer independent: the difference $d = \text{number}[V_{p,q}] - \text{number}[V_{q,p}]$ of the conjugated vertices must be the same in magnitude (but opposite in sign) for the two circles. Therefore, one has to compute the colouring factors for each ring at a fixed difference d and then perform a summation of the product of two colouring factors over d (or, equivalently, over the related variable $D = \frac{1}{2}(r+b+g-|d|)$). The result reads (see appendix C for details)

$$\begin{aligned}\mathrm{Col}_{\mathrm{GUE}}(r,g,b,R,G,B) \equiv l_1 l_2 \sum_{D=\max(r,g,b)}^{\frac{l_1}{2}} \Lambda(D) \\ \times \left\{ \sum_{p=\max(r,g,b)}^{D} \frac{(l_1 - D - p, D-p, p-r, p-g, p-b)}{p} \sum_{q=\max(R-r,G-g,B-b)}^{\frac{l_2-l_1}{2}+D} \right. \\ \left. \times \frac{\left(\frac{l_2+l_1}{2} - D - q, \frac{l_2-l_1}{2} + D - q, q-(R-r), q-(G-g), q-(B-b)\right)}{q} \right\} \\ l_1 \equiv r+g+b \qquad l_2 = R-r+G-g+B-b \\ \Lambda(D) = \begin{cases} 2 & \text{if} \quad D < \dfrac{l_1}{2} \\ 1 & \text{if} \quad D = \dfrac{l_1}{2} \text{ and } \dfrac{l_1}{2} \text{ is integer.} \end{cases}\end{aligned} \tag{38}$$

Brackets $(\alpha_1, \alpha_2, \alpha_2, \cdots) \equiv \frac{(\alpha_1+\alpha_2+\alpha_3+\ldots)!}{\alpha_1!\alpha_2!\alpha_3!\cdots}$ denote the multinomial coefficient.

The colouring factor has much simpler form for the line-diagram. For the example shown in figure 8(*b*), where $g = r + b$; $G = R + B$, Col acquires the following form in GOE and GUE:

$$\mathrm{Col}|_{g=r+b;G=R+B} = \mathrm{Col}_{\mathrm{line}}(r,b)\,\mathrm{Col}_{\mathrm{line}}(R-r, B-b) \qquad \mathrm{Col}_{\mathrm{line}}(a,b) \equiv 2\frac{(a+b)!}{a!b!}. \tag{39}$$

There is no essential difference in the calculation of the Trotter integral for the case of two and three colours. We follow the algorithm explained in appendix B. For *three* colours, the integrand contains a product of *two* 'infusible' $\mathcal{D}_N$ functions. They are converted to the δ-functions and the result of integration with the accuracy of $1/(\tilde{N}\tau)^2$ is

$$\begin{aligned}\mathcal{I}(r,g,b,R,G,B) = 2\pi \frac{\beta}{\sqrt{3}} \frac{1}{(\tilde{N}\tau)^2} \frac{1}{l_1 l_2} \frac{(R-2)!(G-2)!(B-2)!}{(R+G+B-4)!} \\ \times \frac{1}{(r-1)!(R-r-1)!} \frac{1}{(g-1)!(G-g-1)!} \frac{1}{(b-1)!(B-b-1)!}\end{aligned} \tag{40}$$

where the sum over all possible arrangements of the first Trotter segment is done.

To derive the universal factor $\mathcal{V}(k_1,k_2,k_3)$ in equation (32), we have to perform summation over r, g and b accounting for the different distributions of V-matrices over the traces. We recall that the matrices $\hat{V}$ from the first trace enter the Trotter chain with the minus sign. Therefore, the summand must be multiplied by the factor $(-1)^{l_1}$. Unlike the case of two colours, both the colouring factors (37) and (38) and the Trotter integral (40) depend on the distribution of the coloured segments. Thus we arrive at the sum:

$$\mathcal{V}(k_1,k_2,k_3) = \sum_{r=1}^{R-1}\sum_{g=1}^{G-1}\sum_{b=1}^{B-1}\{(-1)^{r+g+b}\mathcal{K}(r,g,b,R,G,B) \times \mathcal{I}(r,g,b,R,G,B)\}$$

which turns out to be rather cumbersome. Amazingly, these summations can be done analytically and we finally find the correction $\tilde{K}_2$ to the spectral form-factor:

$$\tilde{K}_2 = \frac{\sqrt{3}\beta}{3} \sum_{k_1,k_2,k_3=0}^{\infty} (-1)^{k_1+k_2+k_3} C_\beta^{(3)}(k_1,k_2,k_3)\, \mathcal{R}_N(k_1,k_2,k_3) x^{2(k_1+k_2+k_3)-2} \tag{41}$$

where $\mathcal{R}_N(k_1,k_2,k_3)$ is given by equation (33), $x \equiv N|\tau|b$ and the coefficients are

$$\begin{aligned} C_{\beta=1}^{(3)} &= -\frac{\Gamma(k_1+k_2+k_3)}{\Gamma(k_1+k_2+k_3-3/2)} \frac{\Xi_{\beta=1}(k_1)\Xi_{\beta=1}(k_2)\Xi_{\beta=1}(k_3)}{\Gamma(k_1+k_2)\Gamma(k_2+k_3)\Gamma(k_1+k_3)} \\ \Xi_{\beta=1}(k) &\equiv \frac{2^k\Gamma(k-1/2)\Gamma(k+1/2)}{\sqrt{\pi}\Gamma(k+1)} \end{aligned} \tag{42}$$

$$\begin{aligned} C_{\beta=2}^{(3)} &= (2k_1k_2k_3 - k_1k_2 - k_2k_3 - k_1k_3) \frac{\Xi_{\beta=2}(k_1)\Xi_{\beta=2}(k_2)\Xi_{\beta=2}(k_3)}{\Gamma(k_1+k_2+k_3-3/2)} \\ \Xi_{\beta=2}(k) &\equiv \frac{\Gamma(k-1/2)}{\Gamma(k+1)}. \end{aligned} \tag{43}$$

The correction $\tilde{K}_2$ is governed by the interaction of the three energy levels and results from the summation of 'triangles' and 'lines': All terms with $k_{1,2,3} \geqslant 1$ correspond to the 'triangle' diagrams while the 'line' diagrams are obtained by setting $k_1 = 0$ or $k_2 = 0$ or $k_3 = 0$.

The series in the r.h.s. of equation (41) is three-dimensional and cannot be reduced to a product of one-dimensional series. Therefore an analysis of its behaviour at arbitrary x is not trivial. In the case of GUE, one can represent the function $\Gamma^{-1}(k_1+k_2+k_3-3/2)$ as an integral using the identity [30]:

$$\frac{1}{\Gamma(z)} = \frac{1}{2\pi\mathrm{i}} \int_{-\infty}^{\infty} \frac{\exp(a+\mathrm{i}t)}{(a+\mathrm{i}t)^z}\,\mathrm{d}t \qquad a > 0 \tag{44}$$

and change the order of summations over k_i and integration over t. The real-space summation which is implied in the function $\mathcal{R}_N$ has to be done at the last step. This is an effective tool for the asymptotic analysis of the series (41) in GUE. The case of GOE is more complicated. Numerical and semi-numerical methods are useful here. We will demonstrate an application of equations (41)–(43) to the Rosenzweig–Porter model and to a critical almost diagonal PLBRM in the forthcoming paper [29].

6. The case of crossover: almost unitary Gaussian ensemble

We end the presentation of the method with the consideration of an almost unitary Gaussian RM ensemble: we explore the case of a crossover between GOE and GUE [31] which is close to GUE. To define the almost unitary ensemble we introduce a parameter η into equation (34), which controls an asymmetry for the variance of real and imaginary parts of the hopping elements:

$$\langle V_{s,p} V_{q,r} \rangle = b^2 \mathcal{F}(|s-p|)[\delta_{s,r}\delta_{p,q} + \eta\delta_{s,q}\delta_{p,r}]. \tag{45}$$

In GOE, $V_{s,p}$ is a real number and $\eta_{\mathrm{GOE}} = 1$. In GUE the entries $V_{s,p}$ are complex numbers, where $\Re[V_{s,p}]$ and $\Im[V_{s,p}]$ are statistically independent random variables with equal variances and therefore $\eta_{\mathrm{GUE}} = 0$. Hence the parameter β is implicitly linked with η. An ensemble of RM is almost unitary if $0 < \eta \ll 1$.

A first (trivial) impact of small η on the form-factor arises from the proportionality: $\tilde{K}_1 \sim \sqrt{\beta}$; $\tilde{K}_2 \sim \beta$ (see equations (29) and (41)), which comes from the Trotter integrals. We will concentrate on the other outcome of a deviation from GUE where the non-zero parameter

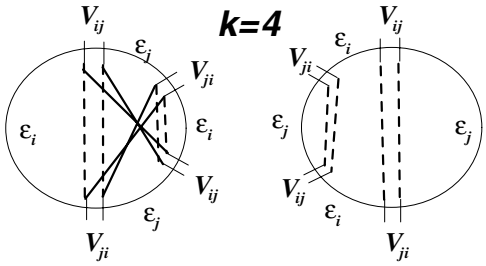

Figure 9. Substitution of the 'non-crossed' connections by the 'crossed' connections: in GUE, only the dotted 'non-crossed' lines are allowed; the diagram with the minimal number of 'crossed' lines is obtained if one substitutes two dotted ILs by the solid ones.

η leads to the appearance of new series in powers of x. We will derive a series that yields a leading in η correction to $\tilde{K}_{1,2}|_{\beta=2}$.

When one performs the Gaussian averaging of V-matrices, V-vertices in the circles can be paired by either 'crossed' or 'non-crossed' connections (see figure 7). Each 'crossed' connection is proportional to η in accordance with definition (45). Therefore, the 'crossed' connections are prohibited in GUE ($\eta = 0$). To explore the leading term in $\eta \ll 1$ in the almost unitary case we have to select the diagrams with a minimal number Cr of 'crossed' ILs. Our main task is to calculate their combinatorics.

We start with the two colours. Let us consider a given distribution of V-matrices over the traces at the fixed parameter k in GUE. There are sets of conjugated vertices: k vertices V_{ij} and k vertices V_{ji}; and there are k connections without crossing. Each 'non-crossed' connection pairs the vertex V_{ij} with its conjugated counterpart V_{ji}. A diagram with the minimal number of 'crossed' ILs is obtained if we choose two 'non-crossed' connections and rearrange them into two 'crossed' connections, see an example in figure 9. The rest $k-2$ ILs remain 'non-crossed'. There are $(k(k-1)/2)^2$ ways to choose two $V_{i,j}$- and two $V_{j,i}$-vertices for the two 'crossed' connections and $(k-2)!$ ways to draw the remaining 'non-crossed' ILs. Therefore, the combinatorial factor for the diagram with the minimal number $Cr = 2$ reads

$$\mathcal{K}_{\eta\ll 1}(k) = 4 \times \frac{k(k-1)}{4} k! \tag{46}$$

where the factor 4 accounts for two different ways to colour each circle by two colours. Substituting equation (46) and the Trotter integral (28) with $\beta = 2$ into the two-colour series (25), we find the correction:

$$\Delta\tilde{K}_1 = \frac{\sqrt{2\pi}}{2}\eta^2 \sum_{k=1}^{\infty} (-1)^k \frac{k}{(k-2)!} \mathcal{R}_N(k) x^{2k-1} \qquad x \equiv N|\tau|b. \tag{47}$$

Each three-coloured diagram in GUE has three sets of conjugated vertices, whose numbers are balanced: number$[V_{i,l}]$ = number$[V_{l,i}] = k_1$, number$[V_{j,l}]$ = number$[V_{l,j}] = k_2$ and number$[V_{i,j}]$ = number$[V_{j,i}] = k_3$. To generate the diagram with the minimal $Cr = 2$ we can repeat the arguments explained above for the case of two colours: a pair of 'non-crossed' connections can be rearranged into a pair of 'crossed' ones successively in the bonds $V_{i,l} \leftrightarrow V_{l,i}$; $V_{j,l} \leftrightarrow V_{l,j}$ and $V_{i,j} \leftrightarrow V_{j,i}$. This procedure results in the combinatorial factor

$$\mathcal{K}|_{\eta\ll 1} = \mathrm{Col}_{\mathrm{GUE}} \frac{k_1(k_1-1) + k_2(k_2-1) + k_3(k_3-1)}{4} \prod_{i=1,2,3} (k_i)! \tag{48}$$

with the colouring factor $\mathrm{Col}_{\mathrm{GUE}}$ defined by equation (38). Therefore, the first correction to GUE takes the form:

$$\Delta\tilde{K}_2 = \frac{2\sqrt{3}}{3}\eta^2 \sum_{k_1,k_2,k_3=0}^{\infty} (-1)^{k_1+k_2+k_3} C^{(3)}_{\eta\ll 1}(k_1,k_2,k_3)\mathcal{R}_N(k_1,k_2,k_3)x^{2(k_1+k_2+k_3)-2} \tag{49}$$

$$C^{(3)}_{\eta\ll 1} = \frac{k_1(k_1-1)+k_2(k_2-1)+k_3(k_3-1)}{4} \times C^{(3)}_{\beta=2}. \tag{50}$$

Another way to insert the 'crossed' ILs into the three-coloured diagram in GUE is to violate the balance of the vertex numbers $\mathrm{number}[V_{i,l}] - \mathrm{number}[V_{l,i}] = d_1$, $\mathrm{number}[V_{j,l}] - \mathrm{number}[V_{l,j}] = d_2$, $\mathrm{number}[V_{i,j}] - \mathrm{number}[V_{j,i}] = d_3$, $d_{1,2,3} = \pm 1, \pm 2\ldots$, and to compensate this violation by the 'crossed' connections. One can prove that the integer parameters d_i are always equal to each other: $d_1 = d_2 = d_3 \equiv d$ (see appendix C). Therefore, the minimal number of 'crossed' connections obtained in this fashion is $Cr|_{d=\pm 1} = 3$ which is, however, larger than $Cr|_{d=0} = 2$ in equations (49) and (50).

7. Examples

In the last section, we give two examples of the application of the general equations (29)–(31), (41)–(43), (47) and (49)–(50) for the corrections $b\tilde{K}_1$ and $b^2\tilde{K}_2$ to the Poissonian form-factor $\tilde{K}_P = 1$. The examples are the Rosenzweig–Porter model with the parameter b depending on the matrix size N and the power-law banded RM with the size-independent parameter b.

7.1. The Rosenzweig–Porter model

Let us consider the Rosenzweig–Porter model with

$$b = \frac{\mathcal{B}}{N} \qquad \mathcal{B} \ll 1 \qquad \mathcal{F}(i-j) = 1. \tag{51}$$

This definition corresponds to an almost diagonal RPRM where a weak perturbation of the diagonal matrix can nevertheless yield a non-trivial level statistics [10].

We note first, that the parameter x does not depend on the matrix size N:

$$x = \tilde{N}|\tau|b = \frac{\tilde{N}}{N}|\tau|\mathcal{B} \equiv T.$$

The ratio $\tilde{N}/N$ is a constant of the order of 1. The product $b^{c-1}\mathcal{R}_N(\{k_i\})$ (c is the number of colours) also has a finite limit at $N \to \infty$. For example, in the case of *two colours*

$$\lim_{N\to\infty}(b\mathcal{R}_N(k)) = \lim_{N\to\infty}\left(\frac{\mathcal{B}}{N}\frac{N-1}{2}\right) = \frac{\mathcal{B}}{2}$$

and equation (29) takes the form:

$$b\tilde{K}_1|_{N\to\infty} = \sqrt{\pi\beta}\mathcal{B}\sum_{k=1}^{\infty}(-1)^k C^{(2)}_{\beta}(k)T^{2k-1} \tag{52}$$

with the coefficients $C^{(2)}_{\beta}(k)$ from equations (30) and (31).

Let us consider for simplicity the complex hopping elements, i.e. $\beta = 2$. The sum over k in equation (52) can be easily calculated and we find:

$$b\tilde{K}_1(T,\beta=2)|_{N\to\infty} = -\sqrt{2\pi}\mathcal{B}T\,\mathrm{e}^{-T^2}. \tag{53}$$

In a similar manner we treat the case of *three colours*, where

$$\lim_{N\to\infty}(b^2\mathcal{R}_N(k_1,k_2,k_3)) = \frac{\mathcal{B}^2}{6}$$

and consequently

$$b^2\tilde{K}_2|_{N\to\infty} = \frac{\sqrt{3}\beta}{18}\mathcal{B}^2\sum_{s=2}^{\infty}(-1)^s \mathrm{C}_\beta(s)T^{2s-2}. \tag{54}$$

The coefficient $\mathrm{C}_\beta(s)$ is given by the sum:

$$\mathrm{C}_\beta(s) = \sum_{k_1,k_2,k_3=0}^{\infty} C_\beta^{(3)}(k_1,k_2,k_3)\delta_{s-(k_1+k2+k_3)} = \sum_{s'=1}^{s}\sum_{k_3=0}^{s'} C_\beta^{(3)}(s-s',s'-k_3,k_3).$$

Here we have introduced the sums of two and three indices: $s = k_1 + k_2 + k_3$, $s' = k_2 + k_3$ and $C_\beta^{(3)}$ is taken from equations (42) and (43). In the case of the complex hopping elements, $\beta = 2$, all summations over k_3, s' and s in equation (54) can be done analytically. The correction to the form-factor takes a simple form:

$$b^2\tilde{K}_2(T,\beta=2)|_{N\to\infty} = -\frac{2\sqrt{3}\pi}{9}\mathcal{B}^2T^2(2T^2-3)\,\mathrm{e}^{-T^2}. \tag{55}$$

The results (53) and (55) are in agreement with the expansion in powers of $\mathcal{B}$ of the exact expression for the form-factor $\tilde{K}(T)$ obtained for $\beta = 2$ in the paper [10].

The case of the real hopping elements, $\beta = 1$, can also be analysed based on the formulae (52) and (54) but the calculations are lengthy and we present them in the forthcoming paper.

7.2. Critical PLBRM

Before giving the example of a critical PLBRM, we would like to discuss generic properties of the virial expansion in the case of the N-independent parameter b and a converging real space sum equation (17). In this case, all corrections to the form-factor $\tilde{K}_m$ are given by the series in powers of the parameter $x = \tilde{N}|\tau|b$ that diverges in the thermodynamic limit. In the leading in $1/N$ approximation in equation (24), where $\mathcal{R}_N(\{k_i\}) = \mathcal{R}(\{k_i\})$, the entire dependence of the spectral form-factor $\tilde{K}(\tau)$ on τ comes only through the dependence on the parameter x. This means that $\tilde{K}(\tau)$ is either τ-independent or divergent (if the series in $\tilde{N}|\tau|b$ determines a function that does not have a finite limit as $\tilde{N}|\tau|b \to \infty$) in the thermodynamic limit.

In order to obtain a dependence on τ for a *finite* limiting spectral form-factor $\tilde{K}(\tau)|_{N\to\infty}$ one has to account for $1/N$-corrections to the real space sum $\mathcal{R}(\{k_i\})$ in equation (24). Rewriting $1/N \sim b|\tau|/(\tilde{N}|\tau|b)$ and absorbing the factor $(\tilde{N}|\tau|b)$ from the denominator into the infinite series, we obtain the correction of order $b\tau$ to the limiting spectral form-factor:

$$\tilde{K}(\tau)|_{N\to\infty} \approx \chi_0 + \chi_1 b|\tau| + \cdots$$

where $\chi_0(b) = 1 + c_{01}b + c_{02}b^2 + \cdots$ is the unfolded level compressibility (see equation (7)); $\chi_1(b) = c_{11}b + c_{12}b^2 + \cdots$, and c_{ij} are numerical coefficients. Thus, the $1/N$ correction to $\mathcal{R}(\{k_i\})$ determines χ_1 and leads to the $b^2|\tau|$ correction in the limiting form-factor. For $b \ll 1$ this correction is small even at the Heisenberg time $\tau \sim 1$. However, it could be important for the *tail* of the two-level correlation function equation (2) at large energy separations ω because it is *non-analytic* in τ.

Now, we illustrate an application of the method developed using an example of a critical almost diagonal PLBRM [14, 16]:

$$b = \mathcal{B} \ll 1 \qquad \mathcal{F}(|i-j|) \equiv \frac{1}{2}\frac{1}{(i-j)^2} \qquad i \neq j. \tag{56}$$

We restrict ourselves to the case $\mathcal{B}\tau \ll 1$ omitting $1/N$-corrections to the real-space sum. The leading term of $\mathcal{R}_N(k)$ takes the following form:

$$\mathcal{R}(k) = \frac{1}{2^k} \lim_{N\to\infty} \sum_{m=1}^{N} \frac{1}{m^{2k}}. \tag{57}$$

Let us substitute expression (57) into equation (29) and explore an asymptotic behaviour $x = \tilde{N}|\tau|\mathcal{B} \to \infty$ of the series (29), (30) and (29), (31) for GOE and GUE, respectively. The simplest route is to change the order of the summations:

$$\tilde{K}_1|_{\mathcal{B}\tau\ll 1} \simeq \frac{2\sqrt{\beta\pi}}{N|\tau|} \sum_{m=1}^{\infty}\sum_{k=1}^{\infty}(-1)^k C_\beta^{(2)}(k) \left(\frac{x}{m\sqrt{2}}\right)^{2k}. \tag{58}$$

The summation over k yields:

$$\tilde{K}_1 \simeq -\frac{\sqrt{\beta\pi}}{N|\tau|} \sum_{m=1}^{\infty} \frac{x^2}{m^2} \exp\left(-\frac{x^2}{2m^2}\right) \begin{cases} I_0\left(\frac{x^2}{2m^2}\right) - I_1\left(\frac{x^2}{2m^2}\right) & \beta = 1 \\ 1 & \beta = 2. \end{cases} \tag{59}$$

Here $I_{0,1}(\cdots)$ are the Bessel functions. The sum over m converges at $m \sim x \gg 1$ therefore it can be converted to the integral over m. After this integration we find the two-colours correction to the level compressibility $\chi_0 \simeq 1 + \mathcal{B} \times c_{01}$:

$$c_{01}|_{\beta=1} = -2 \qquad c_{01}|_{\beta=2} = -\pi. \tag{60}$$

Note, that equation (60) can be reproduced with the help of a heuristic renormalization-group method (compare with [16]).

Using our method it is also easy to derive from equation (47) the correction in the almost unitary case:

$$\Delta c_{01}|_{\eta\ll 1} = \eta^2 \frac{\pi}{16}.$$

We emphasize that it is the behaviour of $\mathcal{F}(|i-j|)$ at large $|i-j|$ that affects the factor $\mathcal{R}(k)$ and governs the asymptotic behaviour of the corresponding series. Depending on it, the two-colour correction may either approach a constant limit or diverge as $N \to \infty$. One can show [29] that: (1) for $\mathcal{F}(|i-j|)$ decreasing *faster* than $1/|i-j|^2$ the two-colour correction *vanishes* in the limit $N \to \infty$; (2) for $\mathcal{F}(|i-j|)$ decreasing *slower* than $1/|i-j|^2$ it is *divergent*. This is the manifestation of the localization–delocalization transition in the spectral statistics. Note that even the case where the series in r.h.s. of equation (29) does not have a finite limit as $N \to \infty$, can be considered by our formalism as long as the correction $\tilde{K}_1(\tau)$ is small at a finite N.

A remarkable feature of the critical PLBRM with $\mathcal{F} \sim 1/|i-j|^2$ in the *three-colour approximation* is the logarithmic divergence $\mathcal{B}^2 \log^2(N|\tau|\mathcal{B})$ of the line- and the triangle-diagrams (see figure 8) at any β. However, in the sum of the line- and the triangle-diagrams, the logarithmically divergent terms of order $\mathcal{B}^2$ cancel out for both GOE and GUE so that $\lim_{x\to\infty}(\tilde{K}_2(\beta = 1, 2))$ is a finite constant of order 1. The sub-leading diverging term *survives strikingly in the three colours correction of the almost unitary ensemble*: $\mathcal{B}^2\Delta K_2 \sim -\mathcal{B}^2\eta^2 \log(N|\tau|\mathcal{B})$. This indicates a failure of the virial expansion for the critical PLBRM as $N \to \infty$ in the crossover between the unitary and orthogonal ensembles and raises a question on the cancellation of the logarithmically divergent corrections of higher orders in b in a pure GOE or GUE. This question deserves a separate detailed study elsewhere.

8. Conclusions

In this paper, we have developed a new method to study the spectral statistics of Hermitian Gaussian random matrices with parametrically small hopping elements $H_{i,j}$ as compared to the diagonal ones: $\langle |H_{i\neq j}|^2\rangle \big/ \langle \varepsilon_k^2\rangle \sim b^2 \ll 1$. We have derived a regular virial expansion of the spectral form-factor in powers of b, where the virial coefficient in front of $b^{\mathcal{A}}$ is given by interaction of $\mathcal{A}+1$ levels.

The expansion is represented by diagrams which are generated with the help of the Trotter formula. We have established the rigorous selection rule for the diagrams, which allows us to account for exact contributions of a given number of resonant and non-resonant interacting levels. Thus the method offers a controllable way to find an answer to the question when a weak interaction of levels can drive the system from localization toward criticality and delocalization.

The method applies to the spectral properties of the random matrices with uncorrelated entries and with a generic dependence of the variance $\langle |H_{i,j}|^2\rangle \equiv b^2\mathcal{F}(|i-j|)$ on the distance $|i-j|$ from the main diagonal. We calculated the corrections governed by interaction of two levels, equations (29)–(31), and three levels, equations (41)–(43), in the cases of GOE, GUE and in the almost unitary ensemble, equations (47), (49) and (50), for an arbitrary function $\mathcal{F}(|i-j|)$. These equations are the main results of the paper. We have demonstrated their application to an almost diagonal Rosenzweig–Porter model and to almost diagonal power-law banded random matrices.

The calculation of the virial coefficients is based on the solution to the combinatorial problem of graph colouring. The solution for the colouring of a single graph is known in a closed form for an arbitrary number of colours [32]. Thus using our method one can, in principle, compute the virial coefficient of an arbitrary order.

Acknowledgments

We are very grateful to Igor Krasovsky, Boris Shapiro and Riccardo Zecchina for useful discussions, to Holger Schanz for his help in combinatorial analysis and to Denis Basko for carefully reading this paper.

Appendix A. The level compressibility

In this appendix, we derive an approximate relation between the level compressibility and the correlation function R. Let us define the two-level correlation function $R_E(\omega)$ centred at energy E:

$$R_E(\omega) = \frac{\left\langle\left\langle \sum_{n,m} \delta(E-\epsilon_n)\,\delta(E-\omega-\epsilon_m)\right\rangle\right\rangle}{\langle\rho(E)\rangle^2}. \tag{A1}$$

In this definition it is assumed that ω is small compared to the total bandwidth, so that $\langle\rho(E)\rangle \approx \langle\rho(E-\omega)\rangle$.

We set apart the diagonal (singular) part in the double sum in numerator of (A1):

$$R_E(\omega) = R_E^{(r)}(\omega) + \frac{\delta(\omega)}{\langle\rho(E)\rangle}. \tag{A2}$$

Then the normalization by $\langle\rho(E)\rangle^2$ ensures that the *regular* part $R_E^{(r)}(\omega)$ depends very weakly on the energy E, except for regions of width $\sim\omega$ near the band edges.

The level number variance can be expressed in terms of the correlation function $R(\omega)$ [24]:

$$\Sigma_2(\bar{n}) = \int_0^{\bar{n}\Delta}\int_0^{\bar{n}\Delta} \left(\langle\rho(E)\rangle^2 R_E(E-E')\right) \mathrm{d}E\,\mathrm{d}E'. \tag{A3}$$

Substituting decomposition (A2) into equation (A3), one finds

$$\Sigma_2(\bar{n}) \simeq \bar{n} + \int_{-\bar{n}\Delta}^{\bar{n}\Delta} \frac{\bar{n}\Delta - |\omega|}{\Delta} R^{(r)}(\omega)\frac{\mathrm{d}\omega}{\Delta} \qquad R^{(r)}(\omega) \equiv R^{(r)}_{E=0}(\omega). \tag{A4}$$

This expression is valid up to the leading order $O(b)$ with respect to $b \ll 1$.

Definition (5) for the level compressibility now yields the following expression:

$$\chi = 1 + \lim_{\bar{n}\to\infty} \int_{-\bar{n}}^{\bar{n}} \mathrm{d}s \lim_{N\to\infty} R^{(r)}(s\Delta). \tag{A5}$$

Using definition (A1), formula (A2) and the identity

$$\int_{-\infty}^{+\infty} \mathrm{d}E \int_{-\infty}^{+\infty} \mathrm{d}\omega \langle\!\langle \rho(E)\rho(E-\omega)\rangle\!\rangle\, \mathrm{e}^{\mathrm{i}\omega t} \equiv \langle\!\langle \mathrm{Tr}\,\mathrm{e}^{\mathrm{i}\hat{H}t}\,\mathrm{Tr}\,\mathrm{e}^{-\mathrm{i}\hat{H}t}\rangle\!\rangle$$

we derive a useful relation:

$$\frac{1}{N}\langle\!\langle \mathrm{Tr}\,\mathrm{e}^{\mathrm{i}\hat{H}t}\mathrm{Tr}\,\mathrm{e}^{-\mathrm{i}\hat{H}t}\rangle\!\rangle \simeq 1 + \Upsilon \int_{-\infty}^{+\infty} \mathrm{d}s\, \mathrm{e}^{\mathrm{i}st\Delta} R^{(r)}(s\Delta) \tag{A6}$$

which remains valid also in the limit $N \to \infty$.

At $t = t_0 \equiv 1/(\bar{n}\Delta)$, large energy scale $\omega \equiv s\Delta \gg \bar{n}\Delta$ does not essentially contribute to the integral in equation (A6) due to the strong oscillations of the integrand. Hence, we have:

$$\lim_{\bar{n}\to\infty} \int_{-\bar{n}}^{\bar{n}} \mathrm{d}s \lim_{N\to\infty} R^{(r)}(s\Delta) = \lim_{\tau_0\to 0} \int_{-\infty}^{+\infty} \mathrm{d}s\, \mathrm{e}^{\mathrm{i}s\tau_0} \lim_{N\to\infty} R^{(r)}(s\Delta) \qquad \tau_0 \equiv t_0\Delta$$

and using equations (A5) and (A6) arrive at expression (7).

Appendix B. Integration over the Trotter variables

In general, the Trotter integral depends on the number of colours and on the distribution of matrices $\hat{V}$ over the traces. The former defines the number of 'infusible' functions $\mathcal{D}_N$ in the integrand while the number of Trotter variables is determined by the latter. In this appendix, we calculate the integral in the case of two colours at an arbitrary number of coloured segments in the circles determined by the parameter m. The integrand in equation (19) (see section 3.2.2) contains two additive parts reflecting two different possibilities to colour the first segments. Unlike that example, we will use another procedure with the simplification that we will not pay attention to the specific colour of the first segments. The final result of the calculation is not affected by this simplification.

Let us apply the Trotter formula to both traces on the r.h.s. of equation (6) involving two infinitely long Trotter chains of length $n_{1,2} \to \infty$ and let the number of coloured segments in the circles be $2m$ and $2(k-m)$. We recall correct colouring by two colours imposes the restriction that a circle must contain equal number of sectors for each colour. Therefore, the total number of segments for a given colour is k with m segments belonging to the first circle and $k-m$ segments in the second one.

Denote the discrete Trotter variables coming from the first trace as $y_1, y_2, \ldots, y_{2m}$ so that the variables $y_1, y_2, \ldots, y_m$ mark the segments of the first colour while the rest of the variables are attributed to the segments of the second colour. The variables from the second trace are

denoted as $z_1, z_2, \ldots, z_{k-m}$ for the first colour and $z_{k-m+1}, z_{k-m+2}, \ldots, z_{2(k-m)}$ for the second one. Since two neighbouring subsegments separated by the origin of the Trotter chain (instead of the V-vertex) are of the same colour we fuse them and mark by the single Trotter variable.

We rescale the variable introducing the continuous ones: $Y_i = y_i/n_1$, $Z_i = z_i/n_2$. They are normalized as (see equation (15))

$$\sum_{i=1}^{2m} Y_i = \sum_{i=1}^{2(k-m)} Z_i = 1 \qquad Y_i \geqslant 0 \quad Z_i \geqslant 0. \tag{B1}$$

The integrand must be multiplied by the factor:

$$\frac{n_1}{2m}\frac{n_2}{2(k-m)}. \tag{B2}$$

The numerator reflects an invariance with respect to a cyclic permutation of the matrices under the traces while the denominator excludes multiple counting of the equal configurations of V-vertices in the circle.

We follow further the algorithm explained in section 3.2.2 and, accounting for the property (B1) and fusing two $\mathcal{D}_N$ functions as is done in equation (19), the Trotter integral can be presented as

$$\mathcal{I}(k,m) = \frac{1}{2m}\frac{1}{2(k-m)}\int_0^1 \prod_{i=1}^{2m-1} \mathrm{d}Y_i \int_0^1 \prod_{j=1}^{2(k-m)-1} \mathrm{d}Z_j \times \theta\left(1 - \sum_{i=1}^{2m-1} Y_i\right)\theta\left(1 - \sum_{j=1}^{2(k-m)-1} Z_j\right)\mathcal{D}_N\left(\sqrt{2}\sum_{i=1}^{m} Y_i - \sqrt{2}\sum_{j=1}^{k-m} Z_j\right). \tag{B3}$$

Having integrated over all variables but $\tilde{Y} = \sum_{i=1}^{m} Y_i$; $\tilde{Z} = \sum_{j=1}^{k-m} Z_j$, we arrive at

$$\mathcal{I}(k,m) = \frac{1}{4}\int_0^1 \frac{\tilde{Y}^{m-1}(1-\tilde{Y})^{m-1}}{m!(m-1)!}\mathrm{d}\tilde{Y}\int_0^1 \frac{\tilde{Z}^{k-m-1}(1-\tilde{Z})^{k-m-1}}{(k-m)!(k-m-1)!}\,\mathrm{d}\tilde{Z}\,\mathcal{D}_N(\sqrt{2}[\tilde{Y}-\tilde{Z}]) \tag{B4}$$

$$\simeq \sqrt{\beta\pi}\frac{1}{\tilde{N}|\tau|}\frac{1}{m!(m-1)!(k-m)!(k-m-1)!}\frac{(k-2)!}{2^k \times (2k-3)!!}. \tag{B5}$$

At the last step, we sum over the parameter m to account for different distributions of V-matrices over the traces:

$$\mathcal{I}(k) = \sum_{m=1}^{k-1}\mathcal{I}(k,m) = \frac{\sqrt{\beta\pi}}{2}\frac{1}{\tilde{N}|\tau|}\frac{1}{k!(k-1)!}. \tag{B6}$$

Appendix C. Combinatorial coefficient of colouring

To calculate the universal factor $\mathcal{V}(\{k_i\})$ at any number of colours c we need a combinatorial factor of the circles' colouring. V-vertices divide the circles into the segments. The colours, which denote the statistically independent energy levels ε_i, should be distributed over the segments in all possible ways under the condition that all adjacent segments must bear different colours.

Let us start with the colouring of a single circle. The question of our interest was formulated in the appendix of paper [32] as follows: how many permutations of L objects of c different colours (given g_1 objects of the first colour, g_2 objects of the second colour, etc) are there under the condition that no objects of the same colour may stand next to each other?

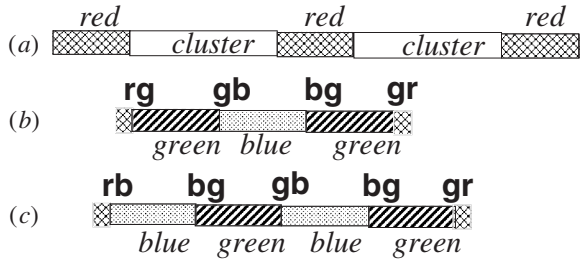

Figure 10. (*a*) An unrolled circle with $r = 2$ and with two clusters of green and blue segments; (*b*) a cluster of odd length; (*c*) a cluster of even length. Pairs of bold letters denote switching of colours at the V-vertices.

We have to supplement it with two additions: (1) we do not distinguish segments of the same colour; (2) we can do cyclic permutations of the segments in the circle. Thereafter, the generic colouring factor can be obtained easily from equation (30) of paper [32]:

$$P_{g_1,g_2,\ldots,g_c}(c) = L(-1)^{L-c}\sum_{n=0}^{\infty}(-1)^n\frac{\partial^{c-1+L}}{\partial x^{c-1+L}}\left[\frac{1}{x}\prod_{i=1}^{c}h_{g_i}(x)\right]\Bigg|_{x=0} \tag{C1}$$

$$h_g(x) = \sum_{s=1}^{g}\binom{g-1}{g-s}\frac{x^s}{s!}. \tag{C2}$$

Equations (C1) and (C2) describe any situation with an arbitrary number of colours and an arbitrary number of segments. Unfortunately, these expressions are cumbersome and are not convenient for a further calculation of the factor $\mathcal{V}$. In this appendix, we will derive a simpler formula for the particular case of three colours, $c = 3$.

We use the notations from section 5 labelling the numbers of the coloured segments by $r = g_1$, $g = g_2$ and $b = g_3$. The first, the second and the third colours will be denoted as 'red', 'green' and 'blue'. Let the colour of the first segment be, for example, red. There are r red segments which separate out r clusters. The clusters contain green and blue segments, which must be arranged in an alternating fashion. The number of segments in the cluster will be referred as the 'length of the cluster'. There are different types of clusters (see figure 10): (1) the clusters with even length that enclose pairs of sectors; (2) the clusters with odd length that enclose pairs as well as one extra segment (either green or blue). We denote the number of these clusters accordingly: n_0, n_g and n_b. The parameters $n_{0,g,b}$ are connected to the numbers of the segments:

$$n_g + n_0 + n_b = r \qquad g - b = n_g - n_b. \tag{C3}$$

First we have to distribute the clusters of three types over r positions. The number of distributions is given by the multinomial coefficient:

$$(n_0, n_g, n_b) \equiv \frac{r!}{n_0!n_g!n_b!}. \tag{C4}$$

Given that each of n_0 clusters of even length contains at least one pair we distribute $b - n_b - n_0 = g - n_g - n_0$ pairs of the segments over r clusters. The corresponding combinatorial factor is

$$2^{n_0}\binom{r + (b - n_b - n_0) - 1}{r - 1} \tag{C5}$$

where 2^{n_0} reflects the possibility of starting the clusters of even length with either a green segment or with a blue one.

The colouring factor $\mathrm{Col}_r(r, g, b)$ for one circle with the red first segment is obtained after summation of the product of equations (C4) and (C5) over the independent number of the clusters, for example, over the parameter n_b in the range $0 \leqslant n_b \leqslant \left[\frac{r+b-g}{2}\right]$. To find the second $\mathrm{Col}_g(r, g, b)$ and the third $\mathrm{Col}_b(r, g, b)$ parts, we have to repeat the same procedure assigning green and blue colours to the first segment of the circle. Equation (37) has been obtained after the summation of all parts[5]:

$$\mathrm{Col}^{(3)}(r, g, b) = \mathrm{Col}_r(r, g, b) + \mathrm{Col}_g(r, g, b) + \mathrm{Col}_b(r, g, b).$$

Equation (38), that is used to calculate the universal factor $\mathcal{V}(k_1, k_2, k_3)$ at $c = 3$ in GUE, has been obtained under an additional condition. Namely, to exclude the 'crossed' connections of the V-vertices each set $\{V_{p,q}, V_{q,p}\}$ must contain an equal number of the 'conjugated' vertices: number$[V_{p,q}]$ = number$[V_{q,p}]$ (see section 5). This restriction applies only to the total number of $V_{p,q}$ and $V_{q,p}$ while the number of conjugated vertices in the same circle is not necessarily balanced. Therefore, colouring of the two circles is not independent.

Let us consider the balance between $V_{p,q}$ and $V_{q,p}$ in more detail. The conjugated vertices inside a cluster with odd length and on its boundary are always balanced (see an example in figure 10(b)). Hence, the clusters of odd length cannot violate the total balance. This is not true for a cluster of an even length: the imbalance between the conjugated vertices is ± 1 for all three sets: $\{V_{i,l}, V_{l,i}\}$; $\{V_{j,l}, V_{l,j}\}$ and $\{V_{i,j}, V_{j,i}\}$ (see an example in figure 10(c)). The sign of the imbalance depends on the colour of the first segment of the given cluster.

Denote the number of clusters of even length, which start with green and blue segments, by $n_0^{(-)}$ and $n_0^{(+)} = n_0 - n_0^{(-)}$, respectively, and introduce a difference $d = n_0^{(+)} - n_0^{(-)} = n_0 - 2n_0^{(-)}$ which will be referred to as 'the number of defects'. It gives the number of imbalanced conjugated vertices of each set in a given circle. Below, the upper indices in $d^{(1)}$ and $d^{(2)}$ will label the number of defects in the first and in the second circles correspondingly.

Since each cluster of even length produces the same imbalance between $V_{p,q}$ and $V_{q,p}$ in all sets of the vertices, the number of conjugated vertices is balanced if

$$d^{(1)} + d^{(2)} = 0. \tag{C6}$$

Equality (C6) must hold true at any combination of the colours of the first segments and expresses the difference of the colouring in GOE and GUE. Equation (37), which is used in GOE, results from an independent summation over the number of defects d_1 and d_2 in each circle. In GUE, we calculate the colouring factor $\widetilde{\mathrm{Col}}_r$ of one circle at fixed d and perform the summation over the number of defects obeying equation (C6):

$$\sum_{d^{(1)}} \sum_{d^{(2)}} \{\widetilde{\mathrm{Col}}_r(r, g, b, d^{(1)}) \times \widetilde{\mathrm{Col}}_r(R - r, G - g, B - b, d^{(2)}) \times \delta_{d^{(1)}, -d^{(2)}}\}.$$

The summand is the product of the colouring factors for the two circles.

To find the expression for $\widetilde{\mathrm{Col}}_r$ we have to sum the product of equations (C4) and a factor similar to equation (C5):

$$\binom{n_0}{n^{(-)}} \times \binom{r + [b - n_b] - n_0 - 1}{r - 1}$$

over the parameter n_b. The factor $\binom{n_0}{n^{(-)}}$ with $n^{(-)} = \frac{n_0 - d}{2} = 0, 1, \ldots$ accounts for the different distributions of the clusters of even length starting with green and blue colours. Equation (38) results from the summation over all combinations of the colours of the first segments.

[5] Formula (37) was obtained with the help of Holger Schanz.

References

[1] Aleiner I L, Brouwer P W and Glazman L I 2002 *Phys. Rep.* **358** 309
[2] Grempel D R, Prange R E and Fishman S 1984 *Phys. Rev.* A **29** 1639
[3] Wigner E P 1958 *Ann. Math.* **67** 325
Dyson F J 1962 *J. Math. Phys.* **3** 1191
[4] Mehta M L 1991 *Random Matrices* (San Diego, CA: Academic)
[5] Guhr T, Muller-Groeling A and Weidenmuller H A 1998 *Phys. Rep.* **299** 189
[6] Vavilov M G and Aleiner I L 2001 *Phys. Rev.* B **64** 085115
Vavilov M G and Aleiner I L 1999 *Phys. Rev.* B **60** R16311
[7] Vavilov M G, Ambegaokar V and Aleiner I L 2001 *Phys. Rev.* B **63** 195313
[8] Fyodorov Y V and Mirlin A D 1991 *Phys. Rev. Lett.* **67** 2405
[9] Rosenzweig N and Porter C E 1960 *Phys. Rev.* **120** 1698
[10] Kunz H and Shapiro B 1998 *Phys. Rev.* E **58** 400
[11] Pandey A 1995 *Chaos Solitons Fractals* **5** 1275
Brezin E and Hikami S 1996 *Nucl. Phys.* B **479** 697
[12] Guhr T 1996 *Phys. Rev. Lett.* **76** 2258
[13] Datta N and Kunz H 2000 *Preprint* cond-mat/0006488
[14] Mirlin A D, Fyodorov Y V, Dittes F M, Quezada J and Seligman T H 1996 *Phys. Rev.* E **54** 3221
[15] Kravtsov V E and Muttalib K A 1997 *Phys. Rev. Lett.* **79** 1913
[16] Evers F and Mirlin A D 2000 *Phys. Rev. Lett.* **84** 3690
Evers F and Mirlin A D 2000 *Phys. Rev.* B **62** 7920
[17] Kravtsov V E and Tsvelik A M 2000 *Phys. Rev.* B **62** 9888
[18] Altshuler B L and Levitov L S 1997 *Phys. Rep.* **288** 487
[19] Levitov L S 1990 *Phys. Rev. Lett.* **64** 547
Levitov L S 1999 *Ann. Phys., Lpz.* **8** 697
[20] Hu B B, Li B W, Liu J and Gu Y 1999 *Phys. Rev. Lett.* **82** 4224
[21] Efetov K 1997 *Supersymmetry in Disorder and Chaos* (Cambridge: Cambridge University Press)
[22] Varga I and Braun D 2000 *Phys. Rev.* B **61** 11859
Cuevas E, Gasparian V and Ortuno M 2001 *Phys. Rev. Lett.* **87** 056601
[23] Ziman J M 1979 *Models of Disorder: the Theoretical Physics of Homogeneously Disordered Systems* (Cambridge: Cambridge University Press)
[24] Chalker J T, Kravtsov V E and Lerner I V 1996 *JETP Lett.* **64** 386
[25] Ndwana M L and Kravtsov V E 2003 *J. Phys. A: Math. Gen.* **36** 3639
[26] Reed M and Simon B 1980 *Methods of Modern Mathematical Physics* (New York: Academic)
[27] Kleinert H 1995 *Path Integrals in Quantum Mechanics, Statistics, and Polymer Physics* (Singapore: World Scientific)
[28] Bollobas B 1998 *Modern Graph Theory* (New York: Springer)
[29] Kravtsov V E and Yevtushenko O in preparation
[30] Gradshtejn I S, Ryzhik I M, Jeffrey A and Zwillinger D 2000 *Table of Integrals, Series, and Products* (San Diego, CA: Academic)
[31] Falko V I and Efetov K B 1994 *Phys. Rev.* B **50** 11267
[32] Berkolaiko G and Keating J P 1999 *J. Phys. A: Math. Gen.* **32** 7827